3rd International Conference on Automation, Control, Engineering and Computer Science (ACECS'16)
Proceedings of Engineering & Technology (PET)
pp. 481-487

Grid Synchronization in Three Phase Power Converters fed by PV system

Fatma Benyoussef[1], Lassâad Sbita[2]

[1,2] Department of Electrical and Control engineering,
National Engineering School of Gabes, Zrig, Gabes 6029, Tunisia
Tel/Fax: +216 75392100
[1] E-mail: fatma.benyoussef14@gmail.com
[2]E-mail: lassaad.sbita@enig.rnu.tn

Abstract— This paper develops a grid synchronization method in three phase power converter fed by PV system. This method is based on a second-order generalized integrator (SOGI) and Frequency-Locked Loop (SOGI-FLL). It is focused on a adaptive filters, developed by a SOGI bloc on the stationary reference frame (αβ). SOGI-FLL is capable to carry out an excellent estimation of the grid voltage symmetrical components in case of faulty grid conditions.
This work analyzes the behavior of the grid synchronization method with faulty grid condition and operating point variation. Simulation results prove the efficiency of the developed method.
Keywords— PV System, GsC, Grid synchronization, second-order generalized integrator, Frequency-Locked Loop.

I. INTRODUCTION

In the last few years, increasing of Photovoltaic (PV) power have made necessary to think about grid connected PV systems, [1],[2]. Actually, Grid synchronization is a famous issue in the connection of power converters to the grid since it allows the power converter and the grid to work in unison [2-3].
Phase angle, amplitude and frequency of the grid voltage are the most critical information. They are used to transform the grid voltage vectors to the corresponding synchronous reference frame. This transformation ensures a dynamic control of the active and reactive power.
To guarantee the grid synchronization, several works develop the phase locked loop algorithm, [4-5], its based on several method such as (PLL Based on a T/4 Transport Delay,[6], PLL Based on the Hilbert Transform,[7], PLL Based on the Inverse Park Transform,[8]…).
The grid stringent requirements provide the need to improve these methods by using some kind of Quadratic Signal Generator (QSG). To simplify the structure of PLL, Second Order Generalized and Frequency-locked loop (SOGI-FLL) has been introduced as a very simple and an effective synchronization [9-10]. Positive- and negative-sequence components (PNSC) is developed in order to analyze the different grid conditions in healthy and safety mode [10-11].
The main contribution of this work is based on grid synchronization in three phase power converters fed by PV generator system. The investigated method consists to estimate the correct angular frequency in order to ensure the grid synchronization; the corresponding positive and negative sequence of the grid is generated in order to analyze the different faulty grid conditions.
The structure of this paper is organized as follows: In section II, the system description is presented and the control strategy is detailed in section III. Grid synchronization method is developed in section IV. The next section focused on the analysis of the performance of grid synchronization method and system control strategy under faulty grid conditions. Finally, this paper is summed up in a conclusion in section VI.

II. SYSTEM DESCRIPTION

The system under study is described in Fig. 1. It's composed of PV generator, DC bus voltage, Grid side Converter (GsC) and three phase converter connected to the grid via a transformer and rl filter. Table I. illustrates the system parameters.

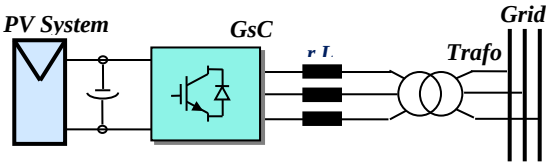

Fig.1 Grid connected PV system topologies

TABLE I.
PARAMETERS SYSTEM

Components	Values
PV generator power	$2.9KW$
Switching frequency	$F_{sw}=10KHz$
Capacitor C_{dc}	$1100\mu F$
Filter rl	$r=0.28\Omega$, $l=1.8mH$
Grid voltage	$U_{rms}=380V$, $50Hz$
DC bus voltage	$610V$

ISSN: 2356-5608

A. *Photovoltaic system*

In direct sunlight, photovoltaic system produced an electrical energy when it is connected to a load [12]. A photovoltaic cell is modeled as a current source connected in parallel with a diode [13]. The simple equivalent circuit of PV cell is illustrated in Fig. 2. It is equipment by a current source which presents the sun irradiation, a P-N junction defined by a diode, series resister R_s and parallel resister R_{sh}, [14].

The Rs is composed by contacts, metal grid and current collecting bus, its value is depends on the number of cells. The R_{sh} is also entitled shunt resistance; its effect is considerably less conspicuous than the series resistance in a PV module.

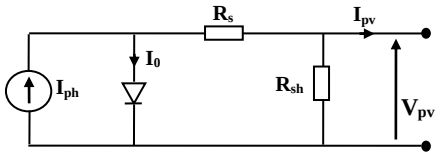

Fig. 2. Equivalent circuit for a photovoltaic cell

The output current I_{pv} of the PV module is expressed as

$$I_{pv} = I_{ph} - I_0[e^{\frac{q(V_{pv}+I_{pv}R_S)}{nKT}} - 1] + \frac{V_{pv} + I_{pv}R_s}{R_{sh}} \quad (1)$$

Where V_{pv} is the output voltage of a solar cell, I_0 present the reverse saturation current, I_{ph} is the photocurrent, K is the Boltzmann's constant, q is the electron charge, T is the junction temperature in Kelvin *(K)* and n present the ideality factor.

The rotation of the earth around the sun and the nonlinear I_{pv}-V_{pv} characteristics of the PV array necessitate the application of maximum power point tracking (MPPT) to the system [15-16]. In this context, grid connected PV systems have become very famous because they do not need battery backup to make MPPT. The system is usually component by two stages. The first stage is used to boost the PV array voltage to generate maximum power from the PV system, the second stage convert this dc power into high quality ac power by the GsC [17].

B. *Grid side Converter*

GsC is composed by semi-conductor IGBTs, it is illustrates in Fig. 3.

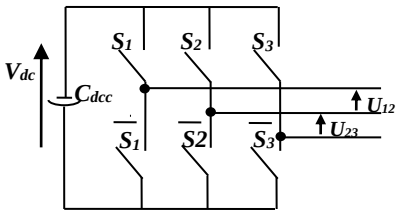

Fig.3. Structure of a three-phase inverter.

Neglecting the dead-time in the IGBT control, the converter model is show by the following equations:

$$\begin{bmatrix} U_{12} \\ U_{23} \end{bmatrix} = \begin{bmatrix} M_1 \\ M_2 \end{bmatrix} V_{dc} \quad (2)$$

Where the variables M_1 and M_2 depend on the signal of the binary switching control, S_i, *{i=1..3}*.

Being,

$$\begin{aligned} M_1 &= S_1 - S_2 \\ M_2 &= S_2 - S_3 \end{aligned} \quad (3)$$

III. CONTROL STRATEGY

The goal of system control strategy, presented in Fig. 4, is to maintain a dc bus voltage constant and to ensure a unity power factor operation. This control is achieved by controlling the inverter output current, I_{Li}, *{i=1..3}*, in the reference rotating frame (d,q).

The frame (d,q) has been oriented on the grid angular frequency, such as the axis 'd' and the vector V_g are confused. So, the voltage $V_{gq} = 0$.

The apparent power S_g is expressed as:

$$S_g = P_g + jQ_g = V_g.I_L^* \quad (4)$$

Where

$$\begin{aligned} I_L^* &= I_{Ld} - j.I_{Lq} \\ S_g &= V_{gd}.I_{Ld} - jV_{gd}.I_{Lq} \end{aligned} \quad (5)$$

I_{Lq} will be null and I_{Ld} provided by an external control loop using a Proportional Integrator controller (PI) in order to ensure a dc link voltage equal to its reference.

Where the P_g and the Q_g are given by the following expressions:

$$\begin{aligned} P_g &= V_{gd}.I_{Ld} \\ Q_g &= -V_{gd}.I_{Lq} \end{aligned} \quad (6)$$

Active power control is ensured via two cascade control loops, they are based on the PI controllers. The external control loop ensures the dc base voltage regulation; its output is the reference of the current direct component, I_{Ld}^*. This one, I_{Ld}^*, is compared to the corresponding measured current, I_{Ld} and injected on the internal PI controller. The output of this controller is the linear term of the direct voltage, V_{Ld}.

Reactive power control is ensured via a PI controller in order the keep the inverse current component, I_{Lq}, null. Its output is the linear term of the inverse voltage component, V_{Lq}.

According to the power circuit dynamics model of the GsC, the references voltages are expressed as

$$\begin{aligned} V_{Ld}^* &= R.I_{Ld} + L\frac{dI_{Ld}}{dt} - w_s.L.I_{Lq} + V_{gd} \\ V_{Lq}^* &= R.I_{Lq} + L\frac{dI_{Lq}}{dt} + w_s.L.I_{Ld} \end{aligned} \quad (7)$$

Linear term | Term of compensation

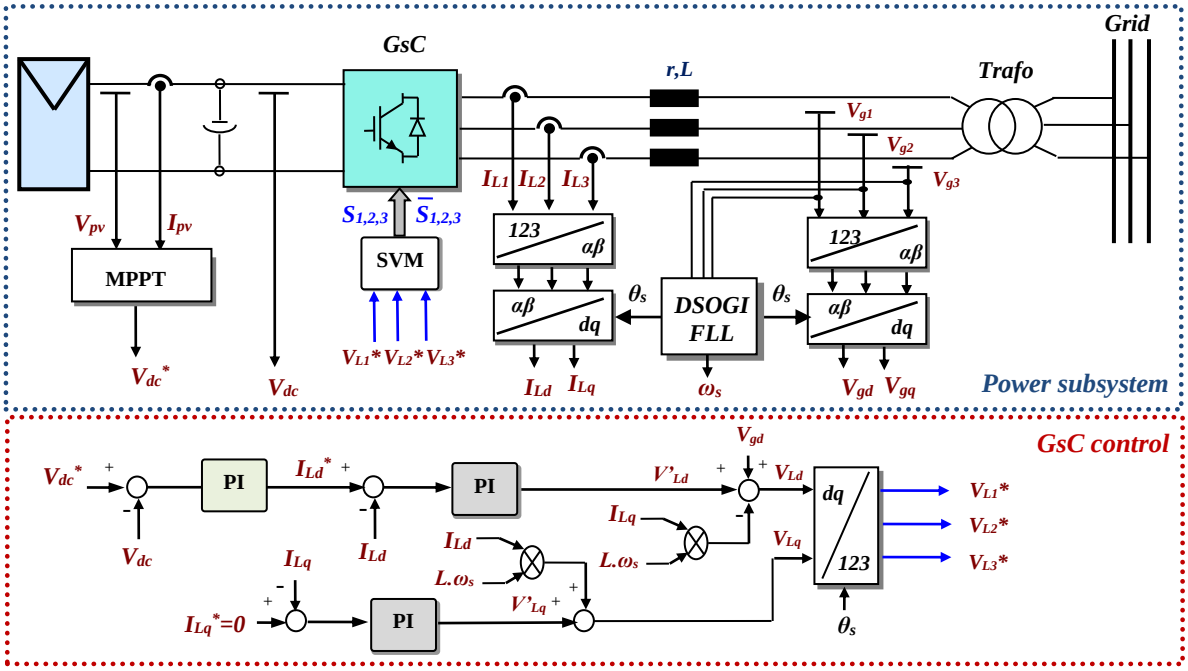

Fig. 4 Control strategy of the system under study

V_{Ld}^{*} and V_{Lq}^{*} is composed by a linear and compensation term, they are also depend on the grid pulsation, w_s.

Park transformation, reference voltages and grid synchronization require a correct determination of the amplitude, phase and angular position of the grid voltage. The next section demonstrates the grid synchronization method.

IV GRID SYNCHRONIZATION METHOD

The synchronization system developed in this work is based on an adaptive filter, where the adjustment frequency is achieved by an SOGI-FLL bloc, [13], [14].

The proposed structure for generating the orthogonal system has a main advantage compared to others methods (i.e. Hilbert Transformation, Transport-Delay, and Inverse Park Transformation). Two main tasks are performed:

- Generating and filtering the orthogonal without delay components;
- The structure has a frequency adaptive.

A. Second Order Generalized Integrator SOGI

Second Order Generalized integrator consists to generate the orthogonal components V' and qV' of the voltage grid V_g, its structure is show in Fig. 5, [18].

The transfer function of the SOGI is expressed in (8). At the resonance frequency, $SOGI(s)$ it is defined by an infinity gain; their outputs and input are in phase. In other frequencies, the phase shift and the gain are nulls

$$SOGI(s)=\frac{V'}{k\varepsilon_g}(s)=\frac{\omega' s}{s2+\omega'^2} \tag{8}$$

Where, the error ε_g is the difference between the V' positive sequence and V_g voltage.

In this structure, two filters have been developed: a pass band filter is defined by the transfer function $D(s)$, it is used to generate the positive sequence, and a pass bas filter is expressed by its transfer function $Q(s)$, it is utilized to generate the negative sequence, see equation (9).

$$D(s)=\frac{V'}{V}=\frac{Ks}{s2+Ks+\omega'^2}$$
$$Q(s)=\frac{qV'}{V}=\frac{K\omega'^2}{s^2+Ks+\omega'^2} \tag{9}$$

Where ω' and K represent respectively the resonance frequency and the gain of the SOGI.

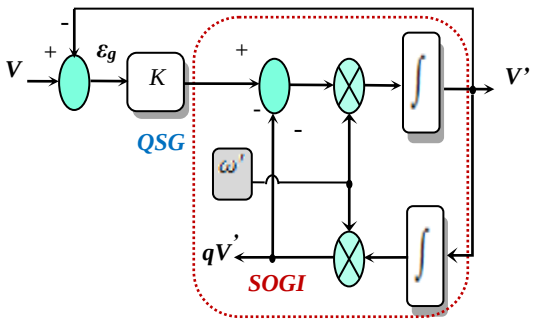

Fig. 5. Structure of SOGI

At different values of gain K, the step response and the Bode diagram of the closed-loop transfer function $D(s)$ are presented in Fig. 6.

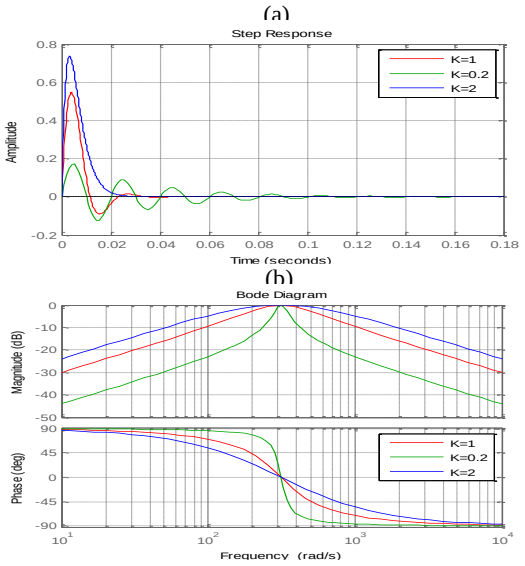

Fig. 6. Step response a) and Bode plot b) of the close loop transfer function D at different values of K

The filtering level depends of the gain K, such as, the filter pass band becomes more limited if K decreases, but the dynamic response of the system becomes slow, see Fig. 6 (a). The Fig. 6 (b) demonstrates that the bandwidth of the closed loop system depends on the coefficient K.

The amplitudes of the sequence V' and qV' are equal, if the resonance frequency of the SOGI bloc, ω', and fundamental frequency, ω_g are equal. So, ω_g must be adjusted to ω'.

A frequency adaptive bloc should be developed in the following paragraph..

B. *Frequency looked loop*

In this case, the adjustment of the resonance frequency of the SOGI is carried out by the FLL structure, which is presented in Fig. 7 [18]. This structure acts on the voltage V_g and its orthogonal component qV' in order to determine the pulsation ω', which must be injected to SOGI bloc.

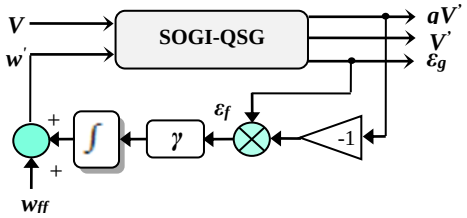

Fig. 7. SOGI-QSG-FLL structure.

where ω_{ff} =134rad/s and ε_f is a negative gain used to eliminate the error in the dc component.

The structure of the grid synchronization system is presented in Fig. 8. So, two SOGI are developed to generate the positive and negative sequence for each output voltage of the Concordia transformation bloc, $V_{\alpha\beta}$, and one FLL bloc is used to generate the grid angular frequency, $\omega_g = \omega'$.

To generate the positive and negative sequences of the three phase grid voltage, a PNSC bloc has been developed, its inputs are the direct and orthogonal signals of the two SOGI.

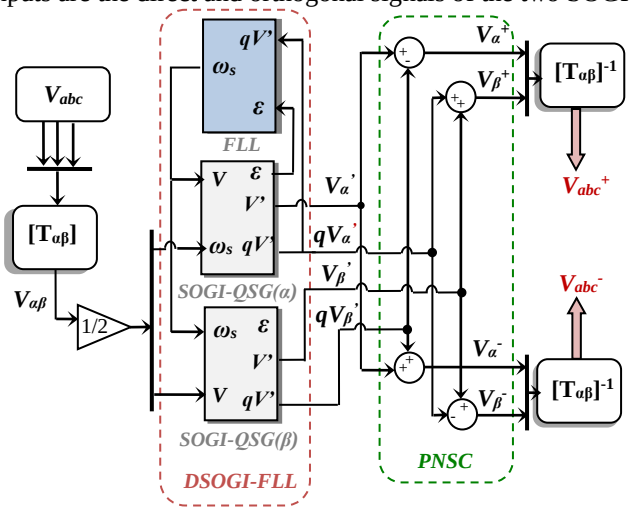

Fig. 8. Positive-/negative-sequence based on the DSOGI-FLL.

C. *Positive and Negative Sequence Components (PNSC)*

Using Lyon's transformation, voltage vector $V_{abc} = \begin{bmatrix} V_a & V_b & V_c \end{bmatrix}^T$ is decomposed by positive and negative components V_{abc}^+ and V_{abc}^-.

$$V_{abc}^+ = \begin{bmatrix} V_a^+ & V_b^+ & V_c^+ \end{bmatrix}^T = \begin{bmatrix} T_+ \end{bmatrix} V_{abc}$$
$$V_{abc}^- = \begin{bmatrix} V_a^- & V_b^- & V_c^- \end{bmatrix}^T = \begin{bmatrix} T_- \end{bmatrix} V_{abc} \quad (10)$$

Where,

$$\begin{bmatrix} T_+ \end{bmatrix} = \frac{1}{3}\begin{bmatrix} 1 & a & a^2 \\ a^2 & 1 & a \\ a & a^2 & 1 \end{bmatrix}; \begin{bmatrix} T_- \end{bmatrix} = \frac{1}{3}\begin{bmatrix} 1 & a^2 & a \\ a & 1 & a^2 \\ a^2 & a^2 & 1 \end{bmatrix},$$

$a = e^{j\frac{2\pi}{3}}$.

The translation from the abc to the $\alpha\beta$ reference frames is given by (8):

$$V_{\alpha\beta} = \begin{bmatrix} T_{\alpha\beta} \end{bmatrix} V_{abc}$$
$$\begin{bmatrix} T_{\alpha\beta} \end{bmatrix} = \sqrt{\frac{2}{3}}\begin{bmatrix} 1 & -\frac{1}{2} & -\frac{1}{2} \\ 0 & \frac{\sqrt{3}}{2} & -\frac{\sqrt{3}}{2} \end{bmatrix} \quad (11)$$

The positive and negative voltage components of the $\alpha\beta$ reference frame are expressed as:

$$V_{\alpha\beta}^+ = \begin{bmatrix} T_{\alpha\beta} \end{bmatrix} V_{abc}^+ = \frac{1}{2}\begin{bmatrix} 1 & -q \\ q & 1 \end{bmatrix} V_{\alpha\beta}$$
$$V_{\alpha\beta}^- = \begin{bmatrix} T_{\alpha\beta} \end{bmatrix} V_{abc}^- = \frac{1}{2}\begin{bmatrix} 1 & q \\ -q & 1 \end{bmatrix} V_{\alpha\beta} \quad (12)$$

With, $q = e^{-j\frac{2\pi}{3}}$.

CORDIC module is applied in order to detect the positive and negative angle (θ_s^+ , θ_s^-) through the following equation.

$$\theta_s^{+-} = \tan^{-1}\frac{V_\beta^{+-}}{V_\alpha^{+-}} \qquad (13)$$

V. PERFORMANCE OF SYSTEM CONTROL STRATEGY UNDER GRID FAULTY CONDITION

In order to demonstrate the performance of system control strategy under grid faulty condition, different simulation tests have been developed.

A. Performance of SOGI-FLL

The Fig. 9(a) shows the evolution of the grid voltages V_{abc} by applying different grid faulty condition, such as Voltage-dip, harmonic distortion (THD=10%) and frequency variation from 50HZ to 60HZ. The faulty condition ranges between t=0.1s to 0.3s.

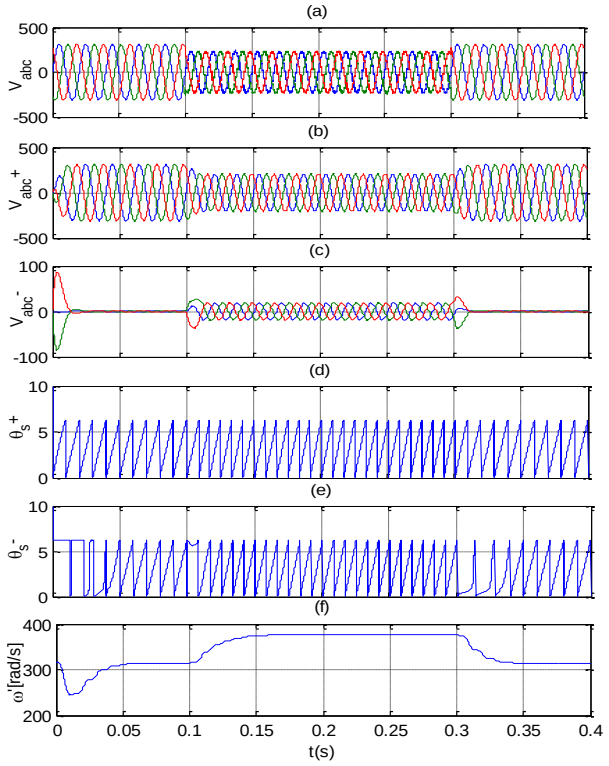

Fig. 9. Response of the DSOGI-FLL in case of multiple disturbances.

The evolution of the positive and negative sequence (V_{abc}^+ , V_{abc}^-) are presented respectively in Fig. 9(b) and Fig. 9(c). The voltage V_{abc}^- are equal to null in safety condition and it have a sinusoidal form in faulty condition.

The phase angles (θ_s^+ , θ_s^-) are shown in Fig. 9(d) and Fig. 9(e). The angular θ_s^+ and θ_s^- track their real values in each operating condition. So, the correct determinations of the phase angle ensures good grid synchronization and the GSC control is performed.

The fig. 9(f) illustrates the evolution of the resonance frequency of the SOGI. It is equal to the angular frequency of the grid. The ω' value is able to overcome without large oscillations in about 40ms.

Simulation tests prove that the SOGI-FLL method able to detect the positive and negative sequence components under very critical conditions.

B. Permormance of GsC control strategy

In order to improve the efficiency of the synchronization method and to evaluate the performance of the GsC control strategy, different simulation tests have been carried out in other operating point, such as a solar irradiance variation and a reference reactive power change. Table II illustrates the simulations parameters.

TABLE II
SIMULATIONS PARAMETERS

Operating point	Simulations parameters	
	$t \in [0 \quad 0.15[$	$t \geq 0.15s$
Solar irradiance	600w/m^2	1000w/m^2
Reference quadrature reference I_{Lq}^*	0A	1A

Fig 10 illustrates the evolution of the dc bus voltage, V_{dc} .

It tracks its reference, V_{dc}^*. So, the system stability is ensured through the action of the V_{dc} controller.

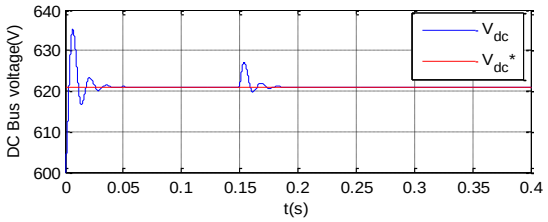

Fig . 10. DC bus voltage variation.

The evolution of the active and reactive powers (P_g , Q_g) is shown in Fig. 11.

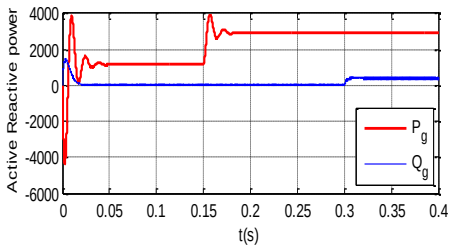

Fig. 11. Instantaneous active and reactive power delivered to the 3-phase utility grid.

The active power is increases at t=0.15s because the reference direct current I_{Ld}^* increases. This one represents the output of the V_{dc} controller. Therefore, in order to maintain Vdc constant, I_{Ld}^* increases in raison to the augmentation of the I_{pv} current at t=0.15s. On the other hand

the reactive power is maintain constant because the current I_{Lq} remains null.

When a I_{Lq} current vary, at t=0.3s, only the reactive power change, see Fig 11 and equation (6).

VI. CONCLUSION

This paper presents the control strategy topology for grid connected PV system and introduces a performed concept for grid synchronization SOGI-FLL-PNSC. The global synchronization method is composed by three fundamental blocs, such as; SOGI block used to generate the orthogonal signal, FLL block that ensures the grid frequency adaptation and PNSC bloc used to analyse the unbalanced and distorted grid voltages by decoupling the network on positive- and negative-sequence components.
Different simulation results have been developed, in safety and faulty grid conditions, in order to ensure the efficiency of the developed grid synchronization method.

ACKNOWLADGE

This work was supported by the Tunisian Ministry of High Education and Research under Grant SPEG_UR11ES82.

REFERENCES

[1] M. A. Eltawil , Z. Zhao, "Grid-connected photovoltaic power systems: Technical and potential problems—A review" , Renewable and Sustainable Energy Reviews, Vol 14, 112–129, 2010.

[2] H. Boumaaraf , A. Talha, O. Bouhali, "A three-phase NPC grid-connected inverter for photovoltaic applications using neural network MPPT" , Vol 49, pp. 1171–1179, September 2015.

[3] N.F. Guerrero-Rodríguez,A. B. Rey-Boué, Luis C. H. d. Lucas, F. Martinez-Rodrigo, "Control and synchronization algorithms for a grid-connected photovoltaic system under harmonic distortions, frequency variations and unbalances" , Renewable Energy, Elsevier, Vol. 80, pp 380–395, August 2015.

[4] F. Gonzalez-Espin, E. Figueres, G. Garcera, "An Adaptive Synchronous-Reference-Frame Phase-Locked Loop for Power Quality Improvement in a Polluted Utility Grid", IEEE Transactions on Industrial Electronics, Vol 59 , NO. 6, 2718 – 2731, October 2011.

[5] D. Dong, B. Wen ; D. Boroyevich, P. Mattavelli, Y. Xue, "Analysis of Phase-Locked Loop Low-Frequency Stability in Three-Phase Grid-Connected Power Converters Considering Impedance Interactions", IEEE Transactions on Industrial Electronics, Vol. 62 , NO. 1 , pp. 310 – 321, juillet 2014.

[6] R. Zhang et al., "A grid simulator with control of single-phase power converters in d-q rotating frame", in Proc. IEEE 33rd Annual Power Electronics Specialists Conference, pp. 1431–1436, 2002.

[7] M. Saitou and T. Shimizu, "Generalized theory of instantaneous active and reactive powers in single-phase circuits based on Hilbert transform", in Proc. IEEE 33rd Annual. Power Electronics Specialists Conference, pp. 1419–1424, 2002.

[8] L. Arruda, S. Silva, and B. J. C. Filho, "Pll structures for utility connected systems", in Proc. IEEE 36th Industrial Application Conference, pp. 2655–2660, October 2001.

[9] S.K.Panda, T.K. Dash, "An improved method of frequency detection for grid synchronization of DG systems during grid abnormalities", International Conference on Circuit, Power and Computing Technologies, Nagercoil, pp. 153 – 157, 2014.

[10] T. Ngo, Q. Nguyen ; S. Santoso, "Detecting positive-sequence component in active power filter under distorted grid voltage", IEEE Power & Energy Society General Meeting, pp. 1-5, July 2015.

[11] M.Fallah, M. Imani, H.M. Kojabadi, M. Abarzadeh, M.T. Bina, L. Chang, " Novel structure for unbalance, reactive power and harmonic compensation based on VFF-RLS and SOGI-FLL in three phase four wire power system", IEEE , Energy Conversion Congress and Exposition (ECCE), Montreal, QC, pp. 6254 – 6260, septembre 2015.

[12] F. Blaabjerg, C. Zhe, and S. B. Kjaer, " Power electronics as efficient interface in dispersed power generation systems", Power Electronics, IEEE Transactions on, vol. 19, no. 5, pp. 1184-1194, Sept.2004.

[13] R. Kadri, J. P. Gaubert, and G. Champenois, " An Improved Maximum Power Point Tracking for Photovoltaic Grid-Connected Inverter Based on Voltage-Oriented Control", Industrial Electronics, IEEE Transactions on, vol. 58, no. 1, pp. 66-75, Jan.2011.

[14] M. G. Villalva, J. R. Gazoli, and E. R. Filho, " Comprehensive Approach to Modeling and Simulation of Photovoltaic Arrays", Power Electronics, IEEE Transactions on, vol. 24, no. 5, pp. 1198-1208, May2009.

[15] M.C. Di Vincenzo, D. Infield, "New maximum power point tracker for photovoltaic systems exposed to realistic operational conditions", Renewable Power Generation, IET, Vol. 8, NO. 6, pp. 629 – 637, August 2014.

[16] S.Lyden, M.E.Haque, A.Gargoom, M.Negnevitsky, "Review of Maximum Power Point Tracking approaches suitable for PV systems under Partial Shading Conditions", IEEE Conference on Power Engineering, Hobart, TAS, pp. 1-6, October 2013.

[17] Z. Weiyi, C. Citro, A. M. Cantarellas, R. Daniel, L. Alvaro, P. Rodriguez, "Tuning of proportional resonant controllers for three phase PV power converters with LCL+trap filter", IEEE , T&D Conference and Exposition, 2014 PES, Chicago, IL, USA, pp 1-6, April 2014.

[18] P. Rodriguez, A. Luna, R. S. Munoz-Aguilar, I. Etxeberria-Otadui, R. Teodorescu, and F. Blaabjerg, "A Stationary Reference Frame Grid Synchronization System for Three-Phase Grid-Connected Power Converters Under Adverse Grid Conditions", IEEE Transactions On Power Electronics, Vol. 27, NO. 1, January 2012.